The Effect of *Gomphonema* and Filamentous Algae Streamers on Hydroelectric Canal Capacity and Turbulent Boundary Layer Structure

J.M. Andrewartha[1], J.E. Sargison[1], and K.J. Perkins[2]

[1]School of Engineering
University of Tasmania, Hobart, Tasmania, 7001 AUSTRALIA

[2]School of Plant Science
University of Tasmania, Hobart, Tasmania, 7001 AUSTRALIA

Abstract

Gomphonema, a freshwater diatom, is currently being studied to determine its effect on the capacity of hydroelectric canals and the structure of turbulent boundary layers. *Gomphonema* is the primary fouling organism present in Tarraleah No.1 Canal (operated by Hydro Tasmania) and was found to cause a 10% reduction in flow carrying capacity. Filamentous algae streamers up to 200mm long have also been observed in the canal. A recirculating water tunnel was used to measure the characteristics of the boundary layer flow over a 997mm x 597mm test plate covered with a biofilm grown in the field in an attempt to better understand the mechanisms for the increase in drag. Mean velocity profiles for the fouled test plate have been compared with results for a smooth test plate.

Introduction

Hydro Tasmania operates 27 hydroelectric power stations with a total installed capacity of over 2500MW. Water is supplied through an extensive water conveyance system comprising of over 50 large dams, and approximately 170km of open conduits and 60km of closed conduits. Extensive biofilm growth occurs on the internal surfaces of many of Hydro Tasmania's canals and pipelines. Biofilms are undesirable biological matter that adheres to a surface, including bacteria and algae, and impedes the flow of water [20].

Biofilms produce extracellular polymer substances (EPS), which are secreted to effectively hold the biofilm together and attach it to the substrate [6]. The EPS is a highly hydrated, three-dimensional structure and constitutes 50-80% of the overall biofilm organic matter. It is due to the secretion of EPS that biofilms obtain their slimy characteristic. The thickness and morphology of biofilms are a function of the hydrodynamic operating conditions through, for example, nutrient transport and the formation of filamentous strands. Similarly, the hydrodynamic conditions depend on the nature of the biofilm [3, 6, 20, 22, 23].

The detrimental effect of biofilms on skin friction has been well established over the last century and the increases in frictional resistance and resultant energy losses due to biofilms are of major concern to industry including hydroelectric power generators, water supply industries and ship owners [5, 14-16, 21, 23]. Much research has been done on the effect of biofilms on drag in the marine environment. Both full-scale ship trials [11, 14] and laboratory studies [13, 15, 22, 23] have shown that the presence of biofilms can have a substantial detrimental effect on skin friction and hence ship performance.

Industrial experience has shown that the accumulation of bacterial deposits in freshwater pipelines and penstocks causes a measured increase in headloss and hence decreased generating efficiency and revenue for hydroelectric schemes. Brett [5] and Barton *et al* [1] measured improved headloss in Hydro Tasmania pipelines after removal of biofilms, provided that the internal surface coating is in good condition. Characklis [8] provides a summary of other cases of reduced capacity in pipelines due to the accumulation of biofilms.

The majority of Hydro Tasmania's open conduits are aging concrete-lined canals and flumes, which are affected by the seasonal growth of photosynthesising algae and harsh weather conditions, which degrade the surface. As a result, the capacity of such canals decreases with time.

Hydro Tasmania and the University of Tasmania have embarked on a multidisciplinary study to investigate the effects of biofouling and surface roughness in water conveyance structures. This paper presents results of a study of Tarraleah No.1 Canal, including a description of the dominant fouling organism, *Gomphonema*, the measured improvements in capacity by physically removing the biofilm, and a detailed boundary layer analysis conducted in a purpose-built laboratory facility.

Schultz [23], and Schultz and Swain [22] compared turbulent boundary layers over natural marine biofilms and a smooth plate using a water tunnel similar to the facility used in the current study. They found an increase in skin friction coefficient of 68% for a slime film of 350μm thick and a 190% increase for a surface dominated by filamentous green algae, when compared to a smooth plate. The results demonstrate the importance of low-form biofilms and the effect of biofilm morphology, thickness and composition on hydrodynamic drag.

Nomenclature

A	Cross-sectional area (m^2)
B	Log law constant
C	Constant for hydraulically rough flow
c_f	Local skin friction coefficient
H	Boundary layer shape factor = δ^*/θ
k_s	Equivalent sand grain roughness (mm)
l	Length of test plate (m)
n	Manning's n friction coefficient
Q	Flow rate (m^3/s)
Re_θ	Momentum thickness Reynolds number = $(U\theta/\upsilon)$
Re_l	Test plate Reynolds number = (Ul/υ)
R_H	Hydraulic radius (m)
S_o	Slope of channel invert
u	Local velocity (m/s)
u'	Velocity fluctuation (m/s)

$u*$	Wall shear velocity $=(\tau_w/\rho)^{1/2}$ (m/s)
u^+	u/u*
Δu^+	Roughness function
U	Freestream velocity (m/s)
y	Distance from wall (m)
y^+	yu*/ υ
δ	Boundary layer thickness (mm)
δ^*	Displacement thickness (mm)
θ	Momentum thickness (mm)
κ	von Karman constant
ρ	Density (kg/m^3)
τ_w	Wall shear stress (Pa)
υ	Kinematic viscosity (m^2/s)

Tarraleah No.1 Canal

Tarraleah No.1 Canal is a 19km long concrete-lined open channel which conveys water from Lake King William to the Tarraleah Power Station in central Tasmania, Australia. It is located approximately 600m above sea level and was commissioned in 1938. The canal is subject to extensive biofilm growth, dominated by the diatom species *Gomphonema*, and is the site of ongoing surface coating trials and microbiological studies.

The canal consists of approximately 12.1km of in-ground trapezoidal canal (Figure 1a), 6.6km of above-ground rectangular flume (Figure 1b) and twin steel inverted siphons which convey the water over a steep gully. The design capacity of the canal is 25.5m^3/s; however, the current capacity is approximately 21m^3/s due to the degradation of the concrete surface and extensive biofilm accumulation. The average velocity is approximately 2m/s. The canal is dewatered and scrubbed annually using rotary brooms to remove as much of the biofilm mat from the concrete surface as possible.

The Tarraleah Power Station consists of six Pelton turbines, providing approximately 90MW. However, due to long term water constraints caused by the decreased capacity of Tarraleah No.1 Canal, the station can only operate at 70-75MW.

Figure 1. Tarraleah No.1 Canal (a) Trapezoidal in-ground canal section. (b) Rectangular above-ground flume section.

Description of Fouling Species (*Gomphonema*)

A common fouling species in open conduits and other illuminated locations is the diatom. Diatoms are microscopic, single-celled algae with silica shells and are prevalent in both marine and freshwater environments. They are commonly the first algae to colonise a freshly submerged surface [6]. Diatoms attach themselves to the surface by the secretion of EPS, which allows them to remain in areas where photosynthesis and nutrient access conditions are optimal [24]. Strong adhesion to the substrate helps to prevent sloughing off by high velocity flows or physical disturbances [6].

The *Gomphonema* species present in Tarraleah No. 1 Canal is a raphid diatom, with cells around 35μm long and 6μm wide (Figure 2a). As with a number of other fouling diatom species *Gomphonema* secretes a mucous stalk which pushes the cells

away from the wall (Figure 2b). It is believed stalking is used to push crowded cells towards better light and nutrient conditions [12]. The stalks observed from the fouling at Tarraleah are hundreds of microns long, tens of times the size of the cell itself. As seen in Figure 2c, stalking is intense and the bulk of the fouling seen on the canal wall is made up of stalk material. Debris, dead cells and other algal cells become trapped in the fouling, creating a dense mat.
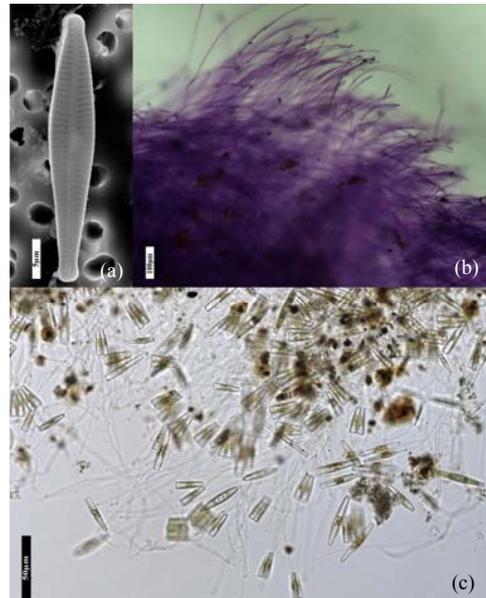

Figure 2 (a) Single *Gomphonema* cell, (b,c) *Gomphonema* mucous stalks

Field Studies

A study was undertaken to determine the maximum capacity of Tarraleah No.1 Canal under both fouled and clean conditions, with a focus on the twin inverted steel siphons which dictate the capacity of the canal. Headloss tests were conducted pre- and post-clean and a hydraulic model of the canal was developed using HEC-RAS (a hydraulic modelling software package). The pre-clean test took place approximately 11 months after the previous canal scrub.

The testing was undertaken at 4 different flow rates for both the pre- and post-clean testing, with nominal capacities of approximately 100%, 90%, 80% and 70%. Freeboard readings were taken at 9 locations in the canal. The flow in each siphon was measured using ultrasonic Panametrics flowmeters and the flow in the canal was gauged using two simultaneous measurements.

A representative Manning's n friction coefficient was derived from the freeboard and canal gauging measurements in both the fouled (n = 0.0142) and clean (n = 0.0137) states using the Chezy-Manning equation (1). These Manning's n values were used in the hydraulic models to predict the maximum capacity of the canal.

$$Q = \frac{1}{n} A R_H^{2/3} \sqrt{S_o} \qquad (1)$$

The measured maximum capacity in the clean condition was 23.4m^3/s and 21.3m^3/s in the fouled condition. This corresponds to a 9.9% increase in capacity as a result of removing the biofilm mat from the wetted surface of the canal and siphons. The test results showed that the cleaning of the inverted siphons was beneficial, as it improved the capacity of the siphons above a flow rate of 17m^3/s. The hydraulic model supported the results obtained from the field testing.

The capacity of the canal will vary considerably depending on the morphology, thickness and composition of the biofilm [3, 22]. The growth of fouling in Tarraleah No.1 Canal is seasonal, with more growth occurring over the warmer summer months. *Gomphonema* is low-form gelatinous biofilm and is expected to cause less hydrodynamic drag than the long green algae filaments which have also been observed to grow in Tarraleah No.1 Canal.

Laboratory Studies

Water Tunnel Set-up
All experimental studies were completed in the UTAS Water Tunnel (Figure 3), located at the School of Engineering, University of Tasmania, Hobart. The UTAS Water Tunnel was constructed specifically for the study of freshwater biofilms and is of closed loop, recirculating design based on the principles of wind tunnel boundary layer research facilities. The facility has the capability to investigate a variety of different surfaces including smooth painted surfaces, artificially roughened surfaces, and biological surfaces. Detailed descriptions of the water tunnel, including the original calibration are given in Barton [3], Barton *et al* [2, 4].

The working section is 2.2m long x 0.6m wide x 0.2m deep with 997mm x 597mm test plates suspended from the lid to form the roof of the working section. A flow conditioner, consisting of two sections of honeycomb and steel mesh separated by 300mm, is installed upstream of the contraction. The two-dimensional contraction has a contraction ratio of 3:1 and is 2m long. The boundary layer is tripped upstream of the working section by a 3mm diameter brass welding rod to ensure a turbulent boundary layer over the test plate. The freestream velocity in the working section ranges between 0.2 – 2.0 m/s. The water temperature is controlled by a cooling system and was set to 15 ± 0.5 °C for the duration of this study. The average water density was 999.0kg/m^3 and the average water viscosity was 0.00114kg/ms.
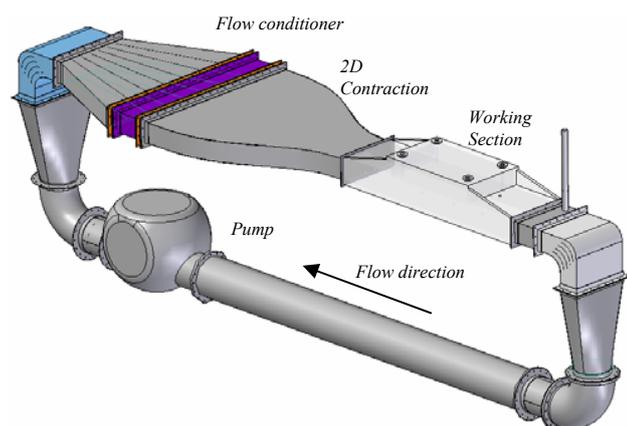

Figure 3. UTAS Water Tunnel Schematic

Test Specimens
Two different test specimens were investigated: a smooth painted reference plate (designated smooth plate) and a fouled sand-grain roughened test plate (designated fouled plate). The test plates were constructed of 3mm thick mild steel with dimensions 997mm x 597mm. The smooth plate was spray painted with four coats of Jotun Jotamastic 87 (two-pack paint), to as smooth a surface as possible. The sand-grain roughened test plate was prepared by applying a tar to the steel plate, and pressing in a fine grit sand mix [4].

Racks are installed in Tarraleah No.1 Canal to allow the insertion of test plates into the canal with the aim to grow flow-conditioned biofilms. The test plates are projected approximately 60mm into the flow away from the wall. The sand-grain roughened test plate was mounted in Tarraleah No.1 Canal in October 2006 and removed in May 2007, allowing a mature biofilm conditioned to flow to develop. The biofilm consisted of a mat of *Gomphonema* and algae streamers up to 200mm long, as shown in Figure 4a. The fouling grown on the test plate (Figure 4a) is believed to be representative of the fouling in the canal, with both the canal wall (Figure 4b) and the test plate exhibiting the brown-coloured *Gomphonema,* and the green-coloured algae streamers. It is expected that the presence of the streamers will cause an additional increase in skin friction coefficient above what would be expected for the low-form gelatinous *Gomphonema*.

The objective of using the smooth plate was to replicate a new or recently refurbished canal or pipeline with a smooth finish. The fouled test plate represents a worst-case scenario where the canal had a significant biofilm layer adhered to a rough aged surface.
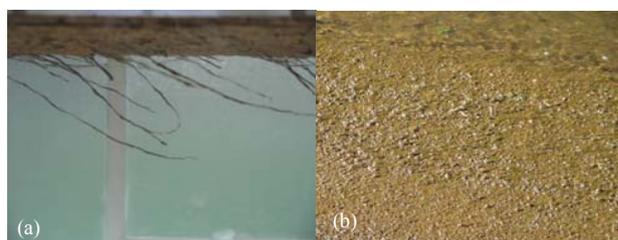

Figure 4. (a) Fouled test plate suspended in water tunnel under zero flow, algae streamers are up to 20cm long. (b) Canal wall fouled with *Gomphonema*.

Experimental Procedure and Data Reduction
Mean velocity boundary layer traverses were completed 95mm downstream from the leading edge of the test plate using a Pitot probe and static wall tapping connected to a Validyne variable reluctance differential pressure transducer (model DP15). The static wall pressure tapping was located in the same plane as the Pitot probe, but offset 50mm longitudinally from the Pitot probe centreline in the spanwise direction to enable the calculation of the local velocity without flow disturbance from the Pitot probe.

The Pitot/static pressure differential was measured at 51 locations throughout the boundary layer on a logarithmic scale, with the probe moved by an automatic linear actuator with a minimum step of 0.01mm. The first measurement was taken with the Pitot probe resting against the test plate and the final measurement was taken in the freestream at 80mm from the wall. Each measurement was recorded at a sampling rate of 1 kHz. All probe measurements were corrected for small temporal changes in test section velocity using the pressure differential across the contraction.

Two methods were used to determine the wall shear velocity, u^*, and the local skin friction coefficient, c_f. The Preston tube method [18] was used for all smooth plate boundary layer profiles. This method is not appropriate for rough or fouled plate measurements, as it requires the Pitot tube to rest flat against a smooth wall. All measurements using the Preston tube method were corrected for the effects of a transverse velocity gradient deflecting the streamlines by using an apparent shift in location of the centre of the probe using the method proposed by McKeon *et al*. [17].

An adaptation of the Clauser chart method [9] developed by Perry *et al.* [19] known as the log-law slope method was used for both the smooth and the fouled test plates. As it is difficult to determine the exact location of the wall for rough or fouled test plates, a wall origin error, ε, is introduced. The method forces a linear log-law region by adjusting ε in small increments until a linear regression line of best fit is determined for plots of u^+ versus $ln(y + ε)^+$ within the log law region. The inner cut-off for the log-law region was set to $y = 50 \, v/u^*$, and the outer cut-off was taken at 15% of the boundary layer thickness, δ [3, 14, 23]. The local skin friction coefficient, c_f, is determined using the slope of the regression line of best fit of u/U versus $ln(yU/v)$, as given in equation 2. The wall shear velocity is then given by equation 3.

$$c_f = 2\kappa^2 (slope)^2 \qquad (2)$$

$$u^* = U \Big/ \sqrt{2c_f^{-1}} \qquad (3)$$

This method has been used successfully on fouled surfaces by Lewthwaite *et al.* [14], Schultz [23], Schultz and Swain [22], and Barton [3]. Due to the introduction of ε, it is expected that the error in the local skin friction coefficient will be greater using the log-law slope method than using the Preston tube method.

Uncertainty Analysis

The uncertainties in the velocity measurements were determined using repeatability tests for a smooth test plate. Ten replicate velocity traces were taken at 5mm from the wall and in the freestream at 80mm from the wall. In order to determine the 95% confidence interval for a single statistic, the standard deviation was multiplied by the two-tailed *t* value (t = 2.262) for 9 degrees of freedom [10, 22]. The uncertainty in the mean velocity is ± 0.7% in the near wall region and ± 0.1% in the freestream. Water temperature is measured to 0.5°C accuracy. The uncertainty in c_f was determined using sequential perturbation analysis and found to be less than 1% for the Preston tube method, and ± 9.5% for the log-law slope method.

Boundary Layer Parameters

A summary of the main boundary layer parameters obtained for the smooth plate are given in Table 1 (Preston tube method) and Table 2 (log-law slope method). The log-law slope method is not widely used for smooth test plates due to the large uncertainty and difficulties in optimising the wall origin error [7, 23]. The process was easier for the fouled plate, as the optimum ε was more obvious than for the smooth plate. The results for the fouled test plate using the log-law slope method are given in Table 3. The boundary layer thickness, δ, is based on the momentum thickness using power law relations (n = 7 for smooth test plate, n = 5 for fouled test plate), as it is less sensitive to accurate wall origin.

For hydraulically rough flow, an equivalent sandgrain roughness height, k_s, can be determined using equation 4, where C = 8.5 for the case of Nikuradse's sand (geometrically similar roughness elements). It is recognised that a single parameter, such as a roughness height, does not adequately describe a compliant surface such as a biofilm [3, 20, 22]. However, a series of parameters that successfully relate the biofilm to the roughness function are yet to be formulated.

$$\frac{u}{u^*} = \frac{1}{\kappa} \ln \left(\frac{y + \varepsilon}{k_s} \right) + C \qquad (4)$$

Figure 5 compares the local skin friction coefficient for smooth and fouled test plates. The equilibrium boundary layer skin friction coefficient is given by equation 5 and is applicable for the range $5 \times 10^5 < Re_l < 10^7$ [25]. Smooth and fouled plate data

measured by Barton [3] in the same facility is shown for comparison. Barton's smooth plate is the same as the smooth plate used in the current study. Barton's fouled plate consisted of filaments between 10 and 30mm long .

$$C_f = \frac{0.0594}{Re_l^{1/5}} \qquad (5)$$

Re_l x 10^6	Re_θ	U (m/s)	δ (mm)	δ^* (mm)	θ (mm)	H	C_f
1.17	3650	1.33	31.9	3.73	3.11	1.20	0.00361
1.35	4610	1.55	34.9	4.10	3.40	1.21	0.00341
1.42	4480	1.63	32.4	3.76	3.15	1.20	0.00348
1.53	5150	1.74	34.6	4.06	3.36	1.21	0.00336
1.65	5380	1.88	33.5	3.93	3.26	1.21	0.00335

Table 1. Boundary layer parameters for smooth test plate using the Preston tube method.

Re_l x 10^6	Re_θ	U (m/s)	δ (mm)	δ^* (mm)	θ (mm)	H	C_f	ε (mm)	Δu^+
1.17	3650	1.33	32.0	3.75	3.12	1.20	0.00358	0.78	-0.21
1.35	4610	1.55	35.0	4.10	3.40	1.21	0.00352	0.99	0.40
1.53	5150	1.74	34.6	4.08	3.37	1.21	0.00352	0.68	0.49
1.65	5380	1.88	33.6	3.94	3.26	1.21	0.00347	0.81	0.49

Table 2. Boundary layer parameters for smooth test plate using the log-law slope method. Note that Re_l and Re_θ are the same as for Table 1.

Re_l x 10^6	Re_θ	U (m/s)	δ (mm)	δ^* (mm)	θ (mm)	H	C_f	ε (mm)	ks (mm)	Δu^+
0.98	3550	1.12	30.3	4.92	3.61	1.36	0.0235	1.23	12.5	14.0
1.18	4250	1.35	30.2	4.86	3.59	1.35	0.0228	1.07	11.2	14.2
1.37	4820	1.57	29.5	4.77	3.51	1.36	0.0204	0.89	9.4	14.0
1.57	5210	1.79	27.9	4.42	3.32	1.33	0.0232	1.19	10.9	14.8

Table 3. Boundary layer parameters for fouled test plate using the log-law slope method.
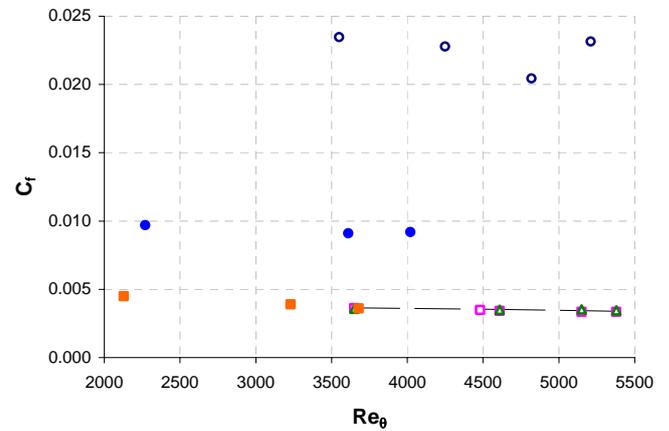

Figure 5. Comparison of local skin friction coefficient data for smooth and fouled test plates. □ Smooth plate (Preston), △ Smooth plate (log-law slope), ■ Barton [3] smooth plate (Preston), ○ Fouled plate (200mm streamers), ● Barton [3] fouled plate (30mm streamers), --- Smooth plate equilibrium.

Mean Velocity Profiles

Boundary layer mean velocity profiles for the smooth test plate are presented in Figure 6, using the Preston tube analysis to determine u^* and c_f. The results shown are for a range of Reynolds numbers based on the length of the test plate and normalised by the wall shear velocity. The results for each Reynolds number collapse well onto the same curve in the log-law region of the boundary layer.
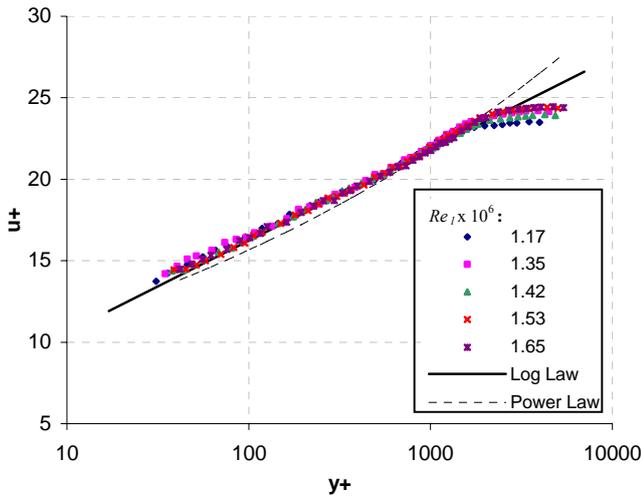
Figure 6. Boundary layer mean velocity profiles for smooth plate with different test plate Reynolds numbers.
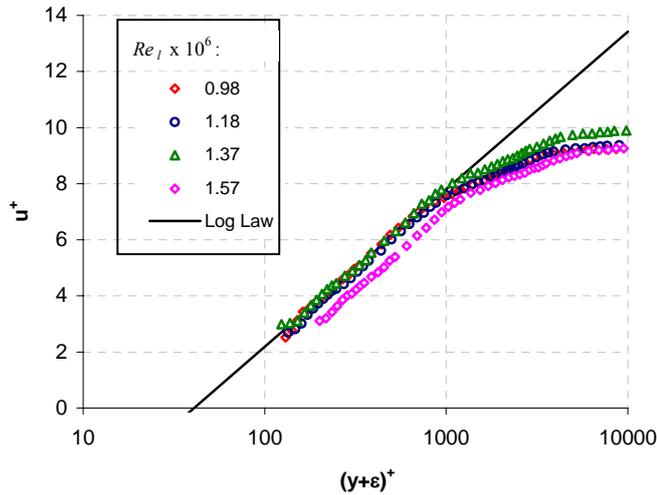

Figure 7. Boundary layer mean velocity profiles for fouled plate with different test plate Reynolds numbers.
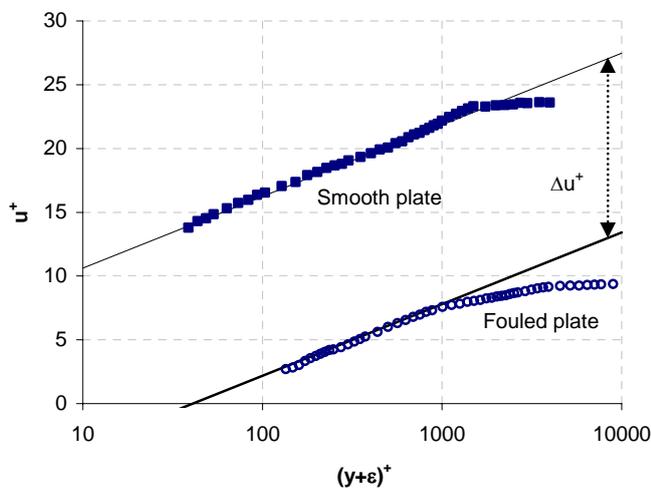

Figure 8. Comparison of smooth and fouled plate boundary layer mean velocity profiles (both determined using the log-law slope method).

The Log Law was fitted to the velocity profiles using equation 6. Note that the von Karman constant, κ, was taken as 0.41 and the smooth wall log law constant, B, was taken as 5.0. The $1/7^{th}$ Power Law was also fitted to the data using equation 7.

$$u^+ = \frac{1}{\kappa} \ln y^+ + B \qquad (6)$$

$$\frac{u}{U} = \left(\frac{y}{\delta}\right)^{\frac{1}{7}} \qquad (7)$$

Boundary layer mean velocity profiles for the fouled test plate are presented in Figure 7. The log law result corresponds to the data at a test plate Reynolds number of 0.98 x 10^6. Figure 8 demonstrates the difference between the smooth and fouled plate boundary layer mean velocity profiles at similar Re_l (1.2 x 10^6).

Discussion

This study aimed to investigate the biofouling species *Gomphonema*, and its effects on hydroelectric canal capacity. *Gomphonema* is the primary fouling organism present in Tarraleah No.1 Canal and has a detrimental impact on the capacity of the canal. The fouling studied in the UTAS Water Tunnel consisted of a dense mat of the low-form gelatinous *Gomphonema* and algae streamers up to 200mm long. The fouling in the canal over the course of the study was also observed to consist of *Gomphonema* and filamentous algae. Ongoing research aims to isolate *Gomphonema* on a test plate so that the effects on skin friction can be measured in isolation from other fouling species, such as the algae streamers.

The skin friction coefficients for both the smooth and fouled plates are shown in Figure 5. The c_f obtained for the smooth plate in the present study is in agreement with the c_f obtained by Barton [3]. As expected, there was a higher degree of uncertainty in c_f when it was determined using the log-law slope method.

The skin friction coefficient for the fouled plate is significantly higher than the skin friction coefficient for the smooth plate, with an increase of 550%. The skin friction results presented here are for the region in the immediate vicinity of the head of the Pitot probe and, as such, represent the local skin friction. The shape factor was higher for the fouled test plate, which was also observed by Schultz for plates fouled with a marine biofilm [23].

The equivalent sandgrain roughness values (k_s) obtained for the fouled plate provide an indication of the effective roughness of the biofilm. It is widely recognised that the effective roughness caused by biofilm growth is considerably greater than the absolute thickness of the biofilm layer, due to the motion of the biofilm under flow conditions [1, 5, 20, 22, 23]. The roughness function, Δu^+ (Figure 8 and Table 3), was found to be approximately 14.3 for the fouled plate. Future work will attempt to relate this roughness function to the characteristics of the biofilm.

Two mechanisms for energy dissipation were observed during the laboratory study:

1. The algae filaments were observed to flutter in three dimensions under flow conditions. It is thought that this movement removes more momentum from the flow than low-form gelatinous biofilms. The reduction in k_s with increase in Reynolds number can be explained by the flattening of the algae filaments towards the wall at higher flow rates.
2. The low-form gelatinous *Gomphonema* was also observed to vibrate under flow conditions. The dense mat structure of the *Gomphonema* significantly impedes the flow in the near wall region, as the water is forced through the biofilm mat.

The length of the algae filaments is a significant point of difference between the results obtained by Barton [3] (algae filaments up to 30mm long and $c_f = 0.0093$) and the results of the present study (algae filaments up to 200mm long and $c_f = 0.022$). The measured skin friction coefficients suggest that the drag exerted by the biofilm is a function of the length of the algae

filaments. This assertion is supported in the literature, with many authors concluding that the composition and morphology of the biofilm determines the hydrodynamic drag [3, 6, 20, 22, 23].

It is recognised that more detailed data is required, consisting of boundary layer profiles at other locations (currently available at 495mm and 865mm downstream of the leading edge of the test plate) and total drag measurements using the force balance attached to the test plate (see Barton *et al.*[4]).

However, combined with the results from the field trial, the boundary layer data provides useful insight into the deterioration of conditions in hydroelectric canals due to the development of biofilms. The field trial measured a 10% increase in capacity due to the removal of the *Gomphonema* mat from the concrete surface lining of Tarraleah No.1 Canal. The boundary layer measurements confirm that the presence of *Gomphonema* and filamentous algae streamers causes an increase in skin friction.

Conclusions

The growth of biofilms in hydroelectric canals and pipelines is a significant problem which extends to more than just the hydroelectric generation industry. A 10% increase in capacity was measured as a result of removing the biofilm mat from the surface of Tarraleah No.1 Canal. Boundary layer measurements on best- and worst-case scenarios demonstrated that an aged fouled surface exhibits significantly greater drag than a smooth painted surface, with a measured increase in local skin friction coefficient of 550%. Multidisciplinary research is continuing at the University of Tasmania to advance the understanding of the biofilm/flow interaction in freshwater conduits, and investigate methods of drag reduction.

Acknowledgments

References

[1] Barton, A. F., Sylvester, M. W., Sargison, J. E., Walker, G. J. and Denne, A. B., *Deterioration of Conduit Efficiency Due to Biofouling*, in 8th National Conference on Hydraulics in Water Engineering, Gold Coast, Australia, 2004.

[2] Barton, A. F., Sargison, J. E., Walker, G. J., Osborn, J. E. and Brandner, P. A., *A Baseline Study of the Effect of Freshwater Biofilms in Hydraulic Conduits*, in XXXI IAHR Congress, Seoul, Korea, Conference Proceedings CD ROM, 2005.

[3] Barton, A. F., *Friction, Roughness and Boundary Layer Characteristics of Freshwater Biofilms in Hydraulic Conduits (PhD Thesis)*, School of Engineering, University of Tasmania, Hobart, 2006.

[4] Barton, A. F., Brandner, P. A., Sargison, J. E. and Walker, G. J., *A Force Balance to Measure the Total Drag of Biofilms on Test Plates*, in 16th Australiasian Fluid Mechanics Conference, Gold Coast, Australia, 2007.

[5] Brett, T. M., Head-Loss Measurements on Hydroelectric Conduits, *ASCE Journal of the Hydraulics Division*, HY1, 1980, 173- 190.

[6] Callow, M. E., A Review of Fouling in Freshwater, *Biofouling*, 7, 1993, 313-327.

[7] Candries, M. and Altar, M., Experimental Investigation of the Turbulent Boundary Layer of Surfaces Coated With Marine Antifoulings, *Journal of Fluids Engineering*, 127, 2005, 219-232.

[8] Characklis, W. G., Attached Microbial Growths - II. Frictional Resistance due to Microbial Slimes, *Water Research*, 7, 1973, 124-.

[9] Clauser, F. H., Turbulent Boundary Layers in Adverse Pressure Gradients, *Journal of the Aeronautical Sciences*, 21, 1954, 91-108.

[10] Coleman, H. W. and Steele, W. G., Engineering Application of Experimental Uncertainty Analysis, *American Institute of Aeronautics and Astronautics Journal*, 33, 1995, 1888-1895.

[11] Haslbeck, E. G. and Bohlander, G., *Microbial Biofilm Effects on Drag - Lab and Field*, in Proceedings 1992 S.N.A.M.E. Ship Production Symposium, 1992.

[12] Johnson, L., Hoagland, K. and Gretz, M., Effects of Bromide and Iodine on Stalk Secretion in the Biofouling Diatom Achnanthes Longipes (Bacillariophyceae), *Journal of Phycology*, 31, 1995, 401-412.

[13] Lewkowicz, A. K. and Das, D. K., Turbulent Boundary Layers on Rough Surfaces With and Without a Pliable Overlayer: A Simulation of Marine Fouling, *International Shipbuilding Progress, Marine Technology Monthly*, 32, 1985, 174-186.

[14] Lewthwaite, J. C., Molland, A. F. and Thomas, K. W., An Investigation into the Variation of Ship Skin Frictional Resistance with Fouling, *Transactions of the Royal Institute of Naval Architects*, 127, 1985, 269-284.

[15] McEntee, W., Variation of Frictional Resistance of Ships with Condition of Wetted Surface, *Transactions of the Society of Naval Architects and Marine Engineers*, 23, 1915, 37-42.

[16] McFie, H., *Power Storage Lakes: Biological Depositions and Energy Losses in Tasmania*, in 47th ANZAAS Congress, Hobart, 1976.

[17] McKeon, B., Li, J., Morrison, J. and Smits, A. J., Pitot Probe Corrections in Fully Developed Turbulent Pipe Flow, *Measurement Science and Technology*, 14, 2003, 1449-1458.

[18] Patel, V. C., Calibration of the Preston Tube and Limitations of its Use in Pressure Gradients, *Journal of Fluid Mechanics*, 23, 1965, 185-208.

[19] Perry, A. E., Schofield, W. H. and Joubert, P. N., Rough Wall Turbulent Boundary Layers, *Journal of Fluid Mechanics*, 37, 1969, 383-413.

[20] Picologlou, B. F., Zelver, N. and Charaklis, W. G., Biofilm Growth and Hydraulic Performance, *Journal of the Hydraulics Division*, HY5, 1980, 733-747.

[21] Pryfogle, P. A., Rinehart, B. N. and Ghio, E. J., Control of Nuisance Algae Growth in Hydropower Distribution Systems, *Waterpower '97*, 1997, 69-75.

[22] Schultz, M. P. and Swain, G. W., The Effect of Biofilms on Turbulent Boundary Layers, *Journal of Fluids Engineering*, 121, 1999, 44-51.

[23] Schultz, M. P., Turbulent Boundary Layers on Surfaces Covered with Filamentous Algae, *Journal of Fluids Engineering - Transactions of the ASME*, 122, 2000, 357-363.

[24] Wetherbee, R., Lind, J. L., Burke, J. and Quatrano, R. S., The First Kiss: Establishment and Control of Initial Adhesion by Raphid Diatoms, *Journal of Phycology*, 34, 1998, 9-15.

[25] White, F. M., *Viscous Fluid Flow*, McGraw-Hill, 1991.